THE PENNSYLVANIA STATE UNIVERSITY
SCHREYER HONORS COLLEGE

DEPARTMENT OF CHEMICAL ENGINEERING

AN EXPERIMENTAL AND COMPUTATIONAL STUDY OF HYDROGENATION ON SUPPORTED METAL CATALYSTS

MEGAN INGALLS
SPRING 2019

A thesis
submitted in partial fulfillment
of the requirements
for a baccalaureate degree
in Chemical Engineering
with honors in Chemical Engineering

Reviewed and approved* by the following:

Michael Janik
Professor of Chemical Engineering
Thesis Supervisor, Honors Adviser

Darrell Velegol
Distinguished Professor of Chemical Engineering
Faculty Reader

* Signatures are on file in the Schreyer Honors College.

ABSTRACT

Organic modifiers can impact heterogeneous catalyst selectivity and activity by altering the adsorption preferences and surface reaction paths. Dually coated supported nanoparticle metal catalysts are prepared, with organic modifiers on both metal particles and their oxide support. Thiols are used to modify metals, with the sulfur head group binding to the surface, while phosphonic acids are used to modify the support. Both thiol and phosphonic acid modifiers form self-assembled monolayers (SAM) on the catalyst surface. Cinnamaldehyde hydrogenation was used to probe the performance of the as-prepared catalysts; the selectivity to cinnamyl alcohol could be potentially improved without significant decreases in activity by coating two self-assembled monolayers on the surface of the catalyst. For the dually coated catalyst, the thiol modifier mainly increased selectivity as was expected from previous work, while the phosphonate coating mainly increased the activity. When adding both thiols and phosphonates to the catalysts in different orders, it was found that the selectivity resembled the second SAM that was added to the catalyst. These changes in selectivity from the second SAM added to the surface were less drastic than the selectivity changes from a single SAM on the surface. For the activity of the catalyst, all of the catalysts with phosphonate coating showed increased activity for cinnamyl alcohol production in comparison to the uncoated Pt/Al_2O_3. The largest increase was seen when phosphonate was added after the thiol, likely from the thiol leaving open the selective active sites that favor cinnamyl alcohol production while the larger amount of phosphonate effected the electronic properties on the surface to increase the rate.

A next potential step in this research is to use organic modifiers to tune the performance of single metal atom catalysts on oxide supports. As an initial step towards this goal, a computational model was developed to investigate hydrogenation reactions on a supported single metal atom catalyst. The catalyst modeled was a single Pt atom catalyst on the 101 surface of anatase TiO_2. Acetaldehyde and trans-2-butene were used to model the functional groups in cinnamaldehyde that can be selectively hydrogenated.

Multiple models were made to observe how the oxidation state of Pt^0, $Pt^{2+,}$ and Pt^{4+} impacts hydrogenation reaction energies. In the Pt^0 models, the adsorption of hydrogen to the surface for the reaction was unfavorable. The absence of hydrogen adsorbed to the surface would cause this catalyst to be unable to hydrogenate trans-2-butene or acetaldehyde. Both the Pt^{2+} and Pt^{4+} catalysts adsorbed hydrogen very strongly; however, this very low energy state that was created made it unfavorable for the hydrogen to leave the surface to hydrogenate the trans-2-butene and acetaldehyde.

TABLE OF CONTENTS

LIST OF FIGURES

ACKNOWLEDGEMENTS

I would like to acknowledge Dr. Janik for his continued support and assistance in my research endeavors over the past four years at Penn State and with the Research Experience for Undergraduates (REU) I participated in. From my REU, I would like to acknowledge Dr. Medlin at the University of Colorado for welcoming and encouraging me in his lab for the summer, along with Patrick Coan and Pengxiao Hao for their daily assistance with my research project. I would also like to thank Dr. Velegol for being a faculty reader of my thesis. Finally, I would like to thank my parents for their continued support in my academic pursuits throughout my lifetime.

Chapter 1

Introduction

Heterogeneous catalysts are commonly used in industry for their high reactivity and their ease of separation, though they usually lack selectivity compared to homogeneous catalysts. Specifically, when used for hydrogenation reactions of α,β-unsaturated carbonyls, the selectivity towards the desired unsaturated alcohol product is low. Supported metals on metal oxides are a useful heterogeneous catalyst for the hydrogenation to unsaturated alcohols.[1] The supported metal can be in the form of nanoparticles spread around the surface of the oxide. One way to tune the selectivity of the nanoparticle catalyst is by modification with self-assembled monolayers (SAMs). SAMs are molecules that align in a single, ordered layer on the surface of a catalyst. SAM modifiers are able to form a consistent layer through a favorable self-limiting assembly.[2] The head group and tail group on these molecules can be tuned for specific reactions. Another way to improve the catalyst is to make a single atom catalyst (SAC) where the metal atoms are highly dispersed on the surface of the metal oxide where there are no interactions between the metal atoms. The higher dispersion allows the individual active sites on the metal to be more specifically tuned. Additionally, the dispersion increases the usefulness of the metal since all atoms are exposed on the surface, unlike metal atoms within nanoparticles, decreasing the cost of the catalyst.[3]

For metal surfaces, thiol SAMs can be used for modification, where the sulfur head group attaches to the surface and the tail can be modified to control selectivity through active site selection, steric interactions, and molecular recognition, as seen in previous studies.[4]

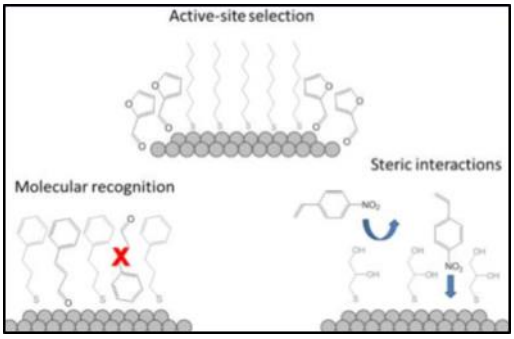

Figure 1: Thiol head groups and tail groups can be tuned for specific functions. Reprinted from ref. 2

In the case of active site selection, the thiols lay on the surface in an ordered manner, attaching to specific types of active sites. The type of active site open to a reactant can impact the product and the rate that it is formed. By controlling the position of the thiols, certain active sites can be opened or blocked, leading to a change in the selectivity towards the different products.

Thiol tails can be used to create steric hindrance, preventing groups of the reactant molecule from reaching the surface. This method has been used with polyunsaturated fatty acids when the desired product is a monounsaturated acid. The intermediates in this reaction are unable to reach the surface, preventing full hydrogenation.[4]

The tail can also be modified to increase the selectivity of a product through noncovalent molecular interactions to orient the reactant. With this method, specific functional groups of the substrate molecule can be directed to the catalytic surface. This effect has been seen most successfully in cinnamaldehyde hydrogenation with 3-phenyl-1-propanethiol as the SAM, where π-π stacking in aromatic rings orients the molecule to favor cinnamyl alcohol.[5]

The metal oxide portion of a supported metal catalyst can be modified with SAMs using phosphonic acid or silane head groups. Phosphonic acids similarly attach to the surface in an ordered manner, with each molecule binding to the surface in up to three locations. Octadecylphosphonic acid typically shows a majority of tridentate binding (three P-O-surface bonds), and 2,3,4,5,6-pentafluorobenzylphosphonic acid binds mostly bidentate.[6,7] Silanes are another molecule used to modify oxide surfaces. Their presence on a surface has shown increased activity for dehydration reactions by

creating more effective active sites though electronic properties.[8] Phosphonates are hypothesized to have similar effects on activity and are more stable on the surface than silanes.[9]

Cinnamaldehyde hydrogenation has been frequently used to represent hydrogenation reactions of α,β-unsaturated aldehydes. The carbonyl product, hydrocinnamaldehyde, is thermodynamically favored, although the unsaturated alcohol, cinnamyl alcohol, is the desired product with many uses in the fragrance and pharmaceutical industries.[10,11,12] Active sites play a crucial role in determining the product from cinnamaldehyde hydrogenation. When the reactant molecule can lay flat on the surface, mostly at terrace sites, it follows the pathway to hydrocinnamaldehyde. The edge sites on that catalyst are positioned in a way that the cinnamaldehyde molecule cannot lay flat, so it instead must stand up with the alcohol directed to the surface which forces the reaction to hydrogenate the alcohol group.

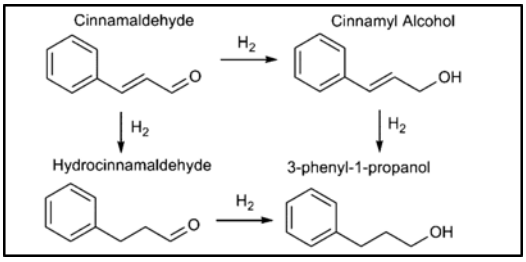

Figure 2 : Cinnamaldehyde reaction pathways. Reprinted from ref 5. Copyright 2014 American Chemical Society.

Within cinnamaldehyde, the two main functionalities for hydrogenation are the carbon-carbon double bond and the carbon-oxygen double bond. These two groups can be modeled with smaller molecules in isolation to compare the effects. A representative molecule for the carbon-carbon double bond is trans-2-butyl since the double bond is in the middle of the molecule, which represents how the molecule must lay flat on the surface of the catalyst for hydrogenation. Acetaldehyde is a representative molecule for the carbon-oxygen double bond with the bond of interest at the end of the molecule. These two chemicals represent the individual chemistry within the full α,β-unsaturated carbonyl.

In addition to SAMs on nanoparticle catalysts, the recent developments in SACs provide an alternative opportunity to improve selective hydrogenation of α,β-unsaturated carbonyls. SACs contain

metal atoms in isolation. The active site contains the metal atom and the surrounding atoms on the metal oxide support. Since each metal atom is in isolation, the active sites are much more uniform on SACs than on nanoparticles where the variability in the size and atom placement makes the active sites on the surface more heterogeneous. Uniform active sites make precisely tuning the catalyst more feasible. An issue with the SACs is complicated synthesis due to the nature of metals forming clusters on the surface. Multiple techniques have been developed for synthesizing metal atoms in insolation on the metal oxide supports including strong electrostatic adsorption that uses pH to obtain a strong electrostatic interaction between the metal atom and the support.[10] Advanced techniques have made the synthesis of uniform SACs possible but adds extra steps beyond the techniques used for depositing nanoparticles to the surface.

Investigations into SACs have shown that the active site chemistry is unique from the chemistry of a nanoparticle, providing an opportunity to take advantage of different reaction conditions to improve selectivity or conversion. When comparing carbon monoxide oxidation on Pt/TiO_2 with varying Pt concentrations, the isolated Pt atoms were the most reactive sites compared to nanoparticle Pt clusters on the surface. It was proposed that the active sites on the Pt SAC were interfacial sites between the metal and metal oxide, leading to the increase in reactivity.[13] On Ru/TiO_2, the selectivity and the turnover frequency for carbon dioxide reduction varied as the ratio of nanoparticle and SAC sites varied, showing that the catalytic properties of the site change based on the form of the metal present.[14]

SACs have been used to catalyze hydrogenation reactions. Au/ZrO_2 catalyzed the hydrogenation of 1,3-butadiene. The SAC active sites were more active than the Au nanoparticle active sites on a comparable catalyst for the reaction.[15] The selective hydrogenation of styrene and acetylene was improved with SAC of Pd/Cu where the isolated Pd atom decreased the adsorption barrier for hydrogen on the surface, while also decreasing the desorption barrier for hydrogen leaving the surface to complete the hydrogenation reaction.[16] A SAC of Pd/mpg-C3N4 selectively hydrogenated 1-hexyne to hexene with higher rates of reaction than other nanoparticle catalysts.[17]

The purpose of this project is to experimentally investigate the effects of adding SAMs to the surface of nanoparticle catalysts and computationally investigate using a single atom catalyst for selective hydrogenation.

In the experimental study, the goal is to observe the effects of using two SAMs, specifically a thiol SAM and a phosphonate SAM, on the same metal oxide supported catalysts for the selective hydrogenation of cinnamaldehyde. The project thus far has focused on using 1-octadecanethiol and 2,3,4,5,6-pentafluorobenzylphosphonic acid as the two monolayers. Since the thiol has a long alkyl chain in its structure, and the phosphonate has a fluorinated benzene ring in its tail, the layers give very distinct IR signals at different wavenumbers. This distinction is important to ensure a successful deposition of the two monolayers. Evidence of both on the surface allows for testing the catalyst with reactions, along with opening up the possibility of other thiol and phosphonate combinations in the future.

In the computational study, the purpose is to use density functional theory to model a SAC of Pt/TiO_2 for the hydrogenation reactions within the cinnamaldehyde molecule to study the individual steps of hydrogenation reactions on the surface of SACs. Due to the larger nature of the molecule, two smaller molecules were chosen to represent the functional groups of interest. Trans-2-btuene and acetaldehyde can be separately hydrogenated on the surface of the modeled SAC and the energy barriers of each reaction step can be used to compare the selectivity.

Chapter 2

Experimental SAM Study

Methods

Materials

Pd/Al_2O_3 (5 wt%), Pt/Al_2O_3 (5 wt%), 1-Octadecanethiol (C18), 2,3,4,5,6-Pentafluorobenzylphosphonic acid (F5BnPA), Octadecylphosphonic acid, Tetrahydrofuran (THF), and Hexanes were purchased from Sigma-Aldrich. 1-Octadecane-d_{37}-thiol was purchased from CDN Isotopes.

Pd/TiO_2 was synthesized with a mixture of $Pd(acac)_2$, benzene, and titanium oxide.[11] These were mixed for 1 hour at room temperature, and dried at 50°C, until all of the benzene evaporated. The substance was then reduced with H_2 gas at 250°C for 2 hours.

Precipitation deposition was used to make Pt/TiO_2. The powder obtained was reduced under H_2 at 350°C for 4 hours.

Monolayer Deposition

The desired SAMs of thiols and phosphonates were deposited to the surface of the catalysts to determine a successful method of synthesis for the dually coated catalyst. Catalysts with the various SAM coatings were also made to analyze the surface with the SAMs and to test the catalyst in a reactor. The two SAMs were deposited individually in sequential steps during the synthesis.

To deposit thiols to the surface, the thiol was mixed with hexane to achieve a concentration of 1mM. The desired catalyst was then added to this solution in a 5:1 ratio of catalyst mass (mg) to solvent

volume (mL). This solution was stirred for a few seconds, covered, and left to sit for 12 hours. The solvent was decanted and new hexane was added for 3 hours to rinse the physisorbed thiols. The solvent was decanted afterwards and dried in a desiccator for 30 minutes before use.

For the phosphonic acid deposition, phosphonic acid was added in a 3:1 ratio of phosphonic acid molecules to surface sites available on the metal oxide. The phosphonic acid was dissolved with THF as the solvent and the catalyst was added. The solution was stirred for 16 hours, centrifuged, poured off, and heated at 120°C for 5 hours. The mixture was washed with THF and centrifuged three times to remove any physisorbed phosphonic acid. The catalyst was dried in the oven for 30 minutes or in the hood overnight before being used.

DRIFTS

Diffuse Reflectance Infrared Fourier Transform Spectroscopy(DRIFTS) was used to characterize the catalyst surface, showing the success of the SAM deposition and the level of SAM order.

In the DRIFTS setup, an infrared beam is directed towards the sample, where the light is reflected off of the surface of the sample. The spectrometer then detects the changes in the light from the molecular vibrations to produce an absorbance spectrum. The peaks on the spectrum at specific wavenumbers correspond to certain bond vibrational modes on the surface. Specifically, C-H stretching occurs around 2900 cm^{-1} and aromatic C-F stretching is at 1500cm^{-1}. The order of the wavenumber can be determined by the exact wavenumber, where a slightly lower number indicates a more ordered surface layer.

Reactions

A liquid phase reactor was used to study the selectivity and activity of the dual SAM coated catalyst for the test reaction of cinnamaldehyde hydrogenation. All reactions were run at 50°C, and under 80 psi H_2, with constant stirring. For the uncoated catalysts, 100mg of catalyst were used. For the coated catalysts, up to 200 mg were used. For all reactions, 48 mL ethanol, 5mL THF, and 1mL cinnamaldehyde were added as in similar studies.[1] Samples were taken from the reactor at 0, 2, 5, 10, 17, 25, 35, and 60 minutes during the reaction course through a filter to separate out the catalyst. The eight samples were then analyzed in a gas chromatograph with a flame ionization detector to determine the amounts of each species by comparing to the THF standard.

Reaction rates were calculated by the change in molarity of the products over the change in time for the first 5 minutes of the reaction. Relative turnover frequencies were determined by dividing the calculated rate of cinnamyl alcohol production by the moles of metal catalyst used. Selectivity was determined by dividing the molarity of one product by the sum of the molarities of all products. The total product molarity was divided by the total molarity of the solution to calculate the conversion of the reaction at a specific time.

Results and Discussion

Preparation of Dually Coated Catalysts

Dually coated SAMs were proven to be successful on Pd/Al_2O_3. As shown in Figure 3, the three characteristic vibrational peaks of the C18 coating occurred at 2958 cm^{-1}, 2925 cm^{-1}, and 2857 cm^{-1}. These peaks signify asymmetric methyl stretching, asymmetric methylene stretching and symmetric methylene stretching, respectively. The three peaks indicate the presence of C18 on the surface of the Pd/Al_2O_3 catalyst. A series of larger peaks also occurred in the 1500-1600 cm^{-1} range of the spectra for the F5BnPA coated catalyst. The peaks occur at 1507 cm^{-1}, 1526 cm^{-1}, and 1658 cm^{-1}, representing the vibrational modes for a fluorinated benzene ring. The presence of the peaks signifies F5BnPA on the surface of the catalyst. For the catalysts with both coatings, which were deposited in different orders, there are three peaks in the C-H stretching range and three peaks in the C-F aromatic stretching range. Evidence of the characteristic peaks of both C18 and F5BnPA suggests successful depositions of the two monolayers onto the same catalyst. For the dually coated catalysts, the C18 asymmetric methylene stretching peak occurred at 2928 cm^{-1}. The same wavenumber for each of these combinations for this peak indicates a similar level of order for the monolayer on these catalysts. With no discernable difference in the IR spectrums for the dually coated catalysts, no significant effect from deposition order could be speculated from this data IR data. On the catalyst with only C18, this peak had a wavenumber of 2925 cm^{-1}, which means that the monolayer was more organized on that surface compared to the combination catalysts.

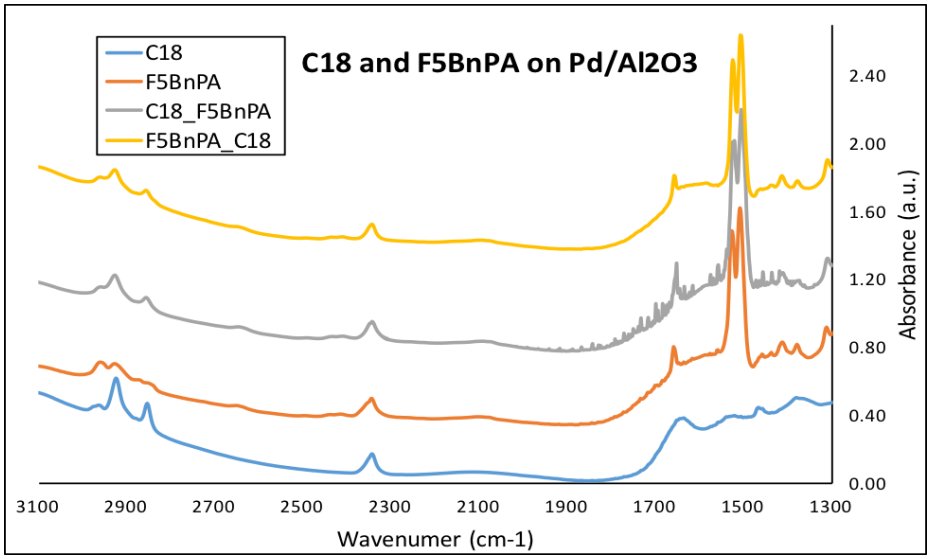

Figure 3: IR data for the thiol, C18, and phosphonate, F5BnPA, added to the surface of a Palladium catalyst separately and in combination.

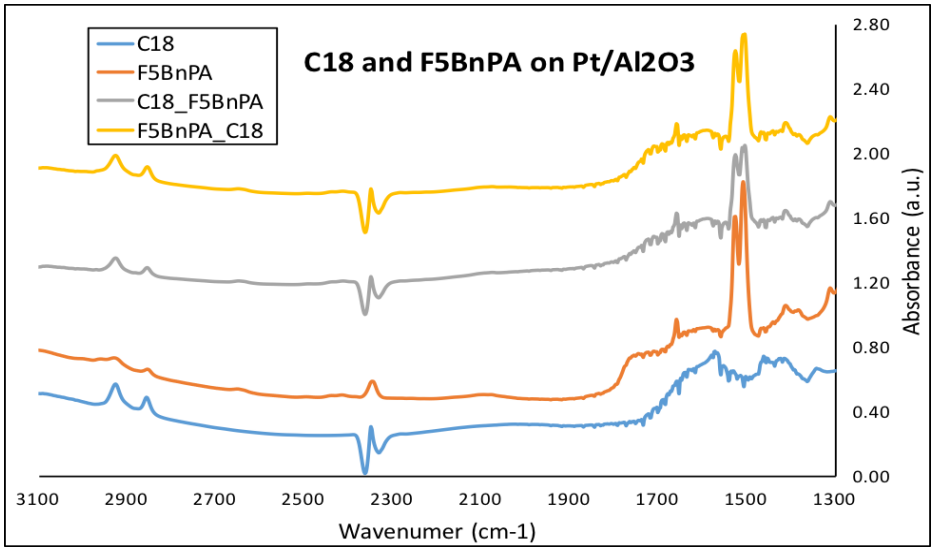

Figure 4: The thiol and phosphonate were also tested with Platinum, where depositions appeared to also be successful.

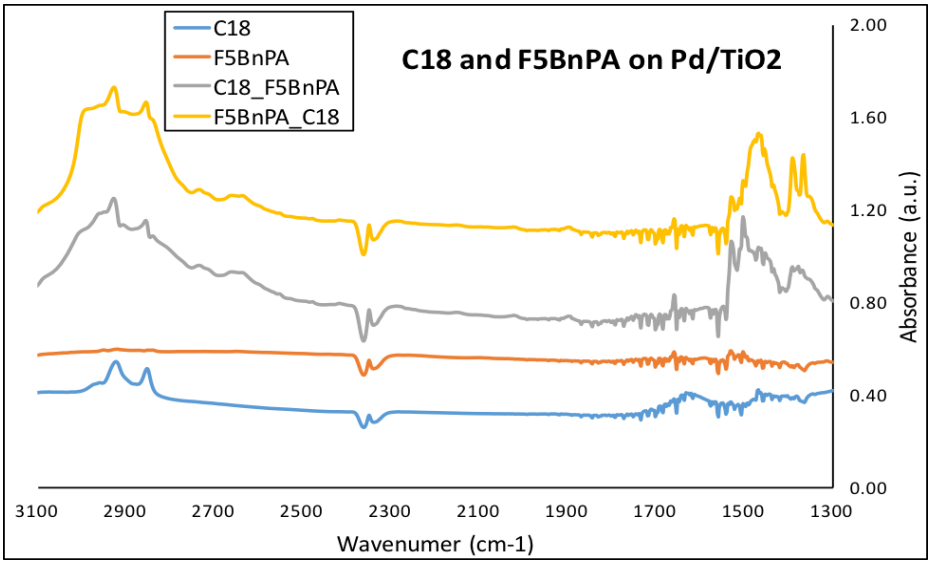

Figure 5: F5BnPA and C18 both are on the surface when the support is changed to titania.

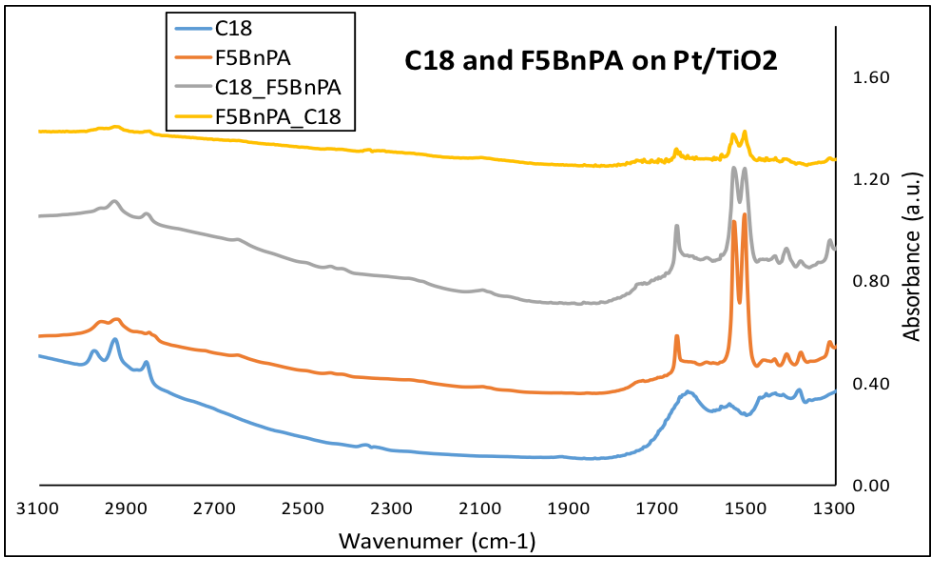

Figure 6: Signals were somewhat weak, but the thiol and phosphonate are visible on the spectra.

After the sequential depositions used to apply the two SAMs appeared successful on Pd/Al_2O_3, the depositions were tested on Pt/Al_2O_3 to investigate the versatility of this method. Again, peaks showed up in the 2900 cm^{-1} range for the C18 coating, and three peaks were apparent in the 1500-1600 cm^{-1} range for the F5BnPA coating. For the dually coated catalysts, both monolayers had peaks in their respective ranges, indicating successful depositions of the two coatings, as seen in Figure 4. In general, compared to the Pd/Al_2O_3 data, the IR signal seemed to be weaker for all of the peaks on the Pt/Al_2O_3. This is likely

the reason for the lack of the third asymmetric methyl stretching peak in all of the C18 depositions. In all of the C18 depositions, the third asymmetric methyl stretching peak was not present. The asymmetric methyl peak is the smallest of the C-H peaks, so it is probably too small of a peak to see, or it could be blended with the asymmetric methylene peak that is the largest.

The depositions of C18 and F5BnPA were also tested on Pd/TiO_2 and Pt/TiO_2 (Figures 5 and 6) to test the effects of changing the support of the catalyst. Both of these catalysts showed evidence of the C18 and F5BnPA on the surface. The peaks looked different from the ones on the alumina catalysts where the signal was stronger, but the wavenumbers for the peaks were in the same ranges. This shows that the monolayers are on the surface, but may not be as ordered as in the other catalysts.

The depositions for the thiol and phosphonate on the same catalyst appeared to be successful for both Pd/Al_2O_3 and Pt/Al_2O_3. The ability to change the metal while still having both SAMs on the surface allows for more versatility in controlling the reactions for which this catalyst could be used. The ability to change the supports was proven on the Pd/TiO_2 and Pt/TiO_2 catalysts, showing that the monolayers will still deposit on other supports, but the IR signals may look slightly different during these changes.

Selectivity of the Dually Coated Catalyst

The desired product in cinnamaldehyde hydrogenation is cinnamyl alcohol. For the uncoated Pt/Al_2O_3, the selectivity ranged from 16%-21% (Figure 7). The selectivity to the desired product cinnamyl alcohol was improved by C18 alone to 24%-36%. It was probably due to blocking of the threefold hollow terrace sites by C18, preventing the cinnamaldehyde from lying flat on the surface. Therefore, more of the cinnamaldehyde tended to have the alcohol group oriented closest to the surface, leading to more hydrogenation of the alcohol.

When F5BnPA alone was added to the surface, the selectivity to cinnamyl alcohol was lowered. The phosphonate attached to the metal oxide portion of the surface, and the tails are possibly in a position

to block the metal edge sites, exposing mostly terrace sites to produce the most common product hydrocinnamaldehyde.

In the combination catalysts, the selectivity was improved from the uncoated Pt/Al_2O_3 catalyst. When C18 was added to the surface after F5BnPA, the selectivity increased more than the selectivity on the catalyst with the F5BnPA added after C18. These increases were less than that with the C18 alone but followed a similar trend.

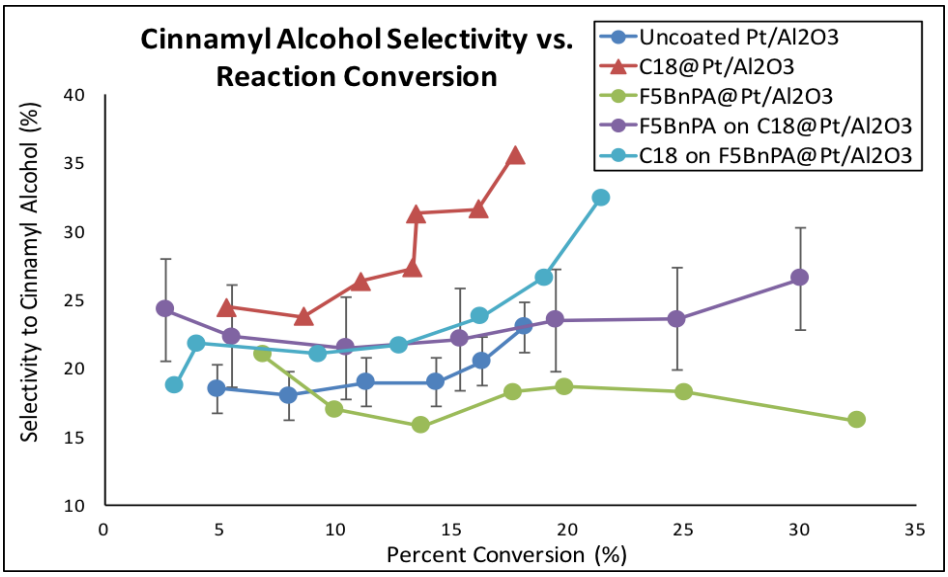

Figure 7: Selectivity data for cinnamyl alcohol on a platinum alumina catalyst.

This trend showed that in general, the selectivity towards cinnamyl alcohol increased as conversion increased, except for the F5BnPA catalyst. The deposition order was seen to make a difference in the performance of the catalysts, hypothetically due to the rinse steps during preparation. Since each deposition requires a number of rinses, the layer added first would be rinsed more than their typical deposition requires. The extra rinses could be enough to remove more of the SAM from the surface, whereas the second deposited layer would still have the typical full SAM layer. This could cause the catalyst with C18 added second to the surface to show higher selectivity, which C18 is known to improve. Additionally, when the phosphonate is added to the surface first, some of the monolayer may attach to the platinum, assisting in blocking the terrace sites to improve the cinnamyl alcohol selectivity.

The different monolayers and combinations of monolayers were also tested in reactions on Pt/TiO_2 catalysts (Figure 8). The general selectivity trend was much different from the alumina supported catalysts. On titania the selectivity decreased with conversion and only improved slightly towards higher conversion. For all of these catalysts, the initial selectivity was the highest.

The uncoated Pt/TiO_2 showed the lowest selectivity. Adding a single layer of F5BnPA slightly increased the selectivity. The C18 monolayer increased the selectivity much more, like on Pt/Al_2O_3. However, on this support the dually coated catalysts showed the highest selectivities. This shows that the dual coatings were beneficial in adding more molecules to the surface to block the terrace sites and leave the edge sites open.

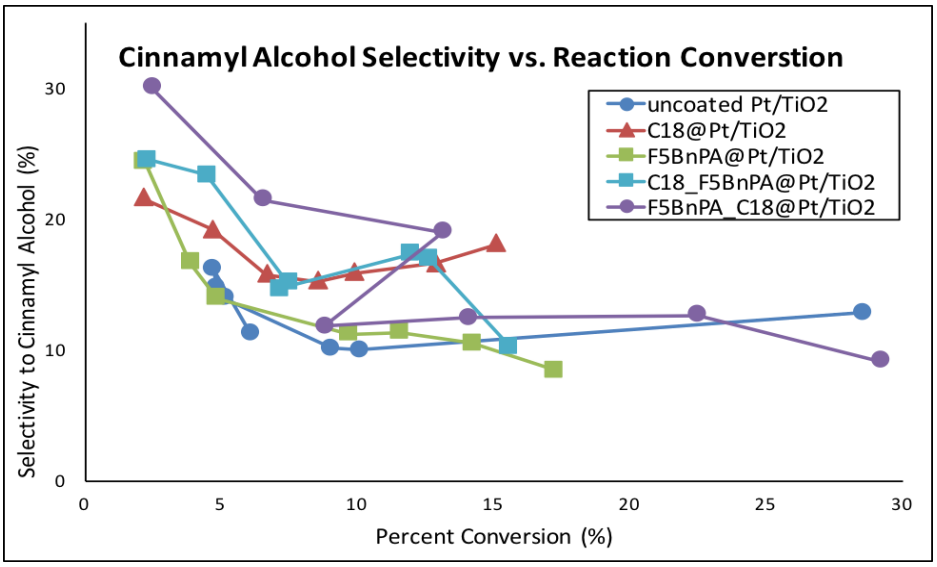

Figure 8: Cinnamyl Alcohol Selectivity on titania supported platinum.

Reactivity of the Dually Coated Catalyst

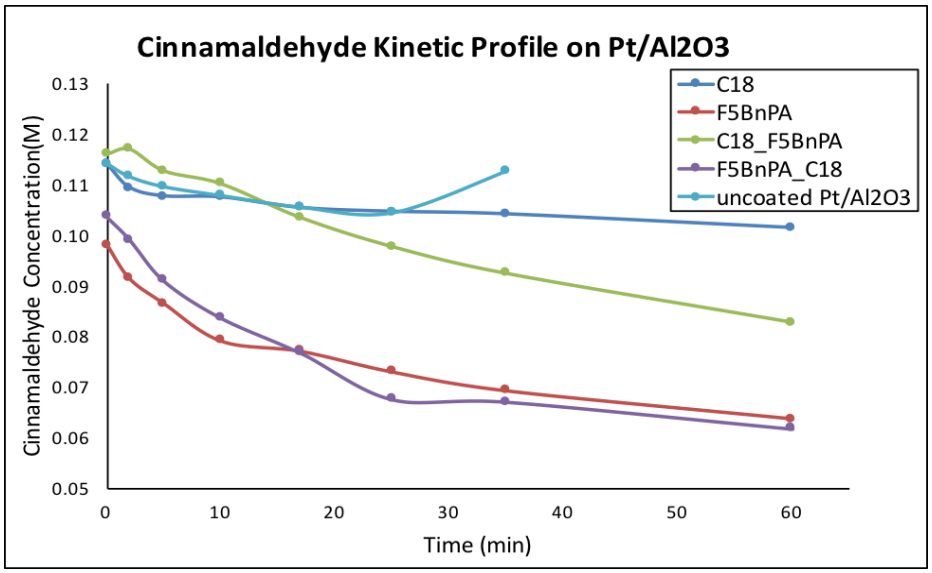

Figure 9: Change in reactant concentration over time.

Both the catalyst with just F5BnPA and the F5BnPA added after C18 had similar rates in the kinetic profile shown in Figure 9. The concentrations of the reactant cinnamaldehyde decreased the fastest of the different catalyst coatings. Both of these likely have the most phosphonic acid on the surface which likely increases the rate the most through electronic properties. The C18 coated catalyst and the uncoated Pt/Al_2O_3 had the lowest rates.

The rates for product production and cinnamyl alcohol production were divided by the moles of metal catalyst to gain a relative idea of turnover frequency, depicted in Figures 10 and 11. Through this calculation it could be seen that all catalysts with the F5BnPA monolayer showed increased activity. When F5BnPA was added after C18, it had a significantly higher turnover frequency for overall production and cinnamyl alcohol production compared to the F5BnPA alone. The C18 on this catalyst likely opened up the edge sites needed to form cinnamyl alcohol, where the phosphonate could then increase the rate at those sites. The F5BnPA alone still increased the turnover frequency, but was not as selective to cinnamyl alcohol.

The catalyst with C18 alone showed a decrease in overall turnover frequency compared to the uncoated catalyst. The turnover frequency was slightly lower than the uncoated catalyst for cinnamyl alcohol production, but it was close since the C18 coating is the most selective. The C18 increases selectivity by blocking the active sites which lowers the activity since there are less available sites for the reaction to take place. Similarly, this is a probable cause for the catalyst with the C18 added after the F5BnPA to have the smallest increase out of the catalysts with phosphonates for the overall turnover frequency. Having a higher amount of C18 on the surface would block more of the active sites and lower the effects of the phosphonate on the surface.

Overall, the C18 lowered the turnover frequency, while F5BnPA improved it. When used in combination, evidence of both effects was present. When looking at the turnover for cinnamyl alcohol specifically, the dually coated catalysts had the highest turnovers. The phosphonic acid on the surface was able to increase the activity of the catalyst. The C18 was also important on the surface so that the increased activity would be towards cinnamyl alcohol rather than the other possible products of the reaction.

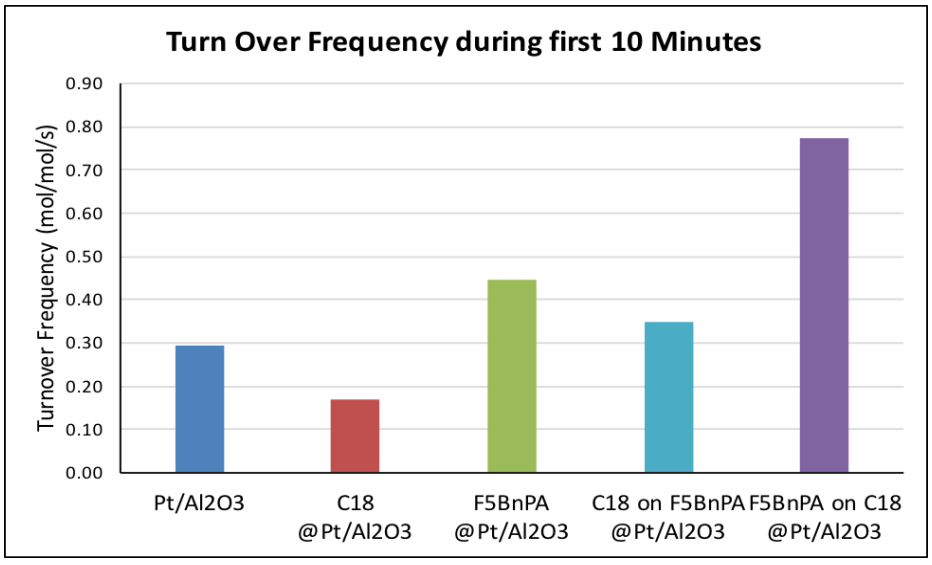

Figure 10: Relative turnover frequencies.

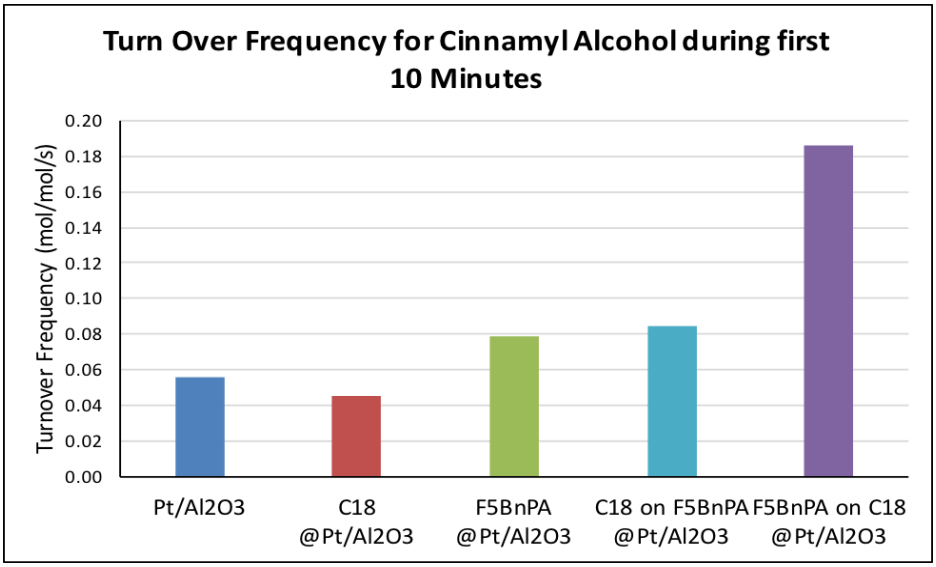

Figure 11: Relative turnover frequencies specifically for cinnamyl alcohol production.

When the support was changed to titania, the rates for the reaction, calculated from the decrease in reactant concentration seemed to be similar (figure 12). Out of the catalysts, the uncoated Pt/TiO_2 had the slowest rate.

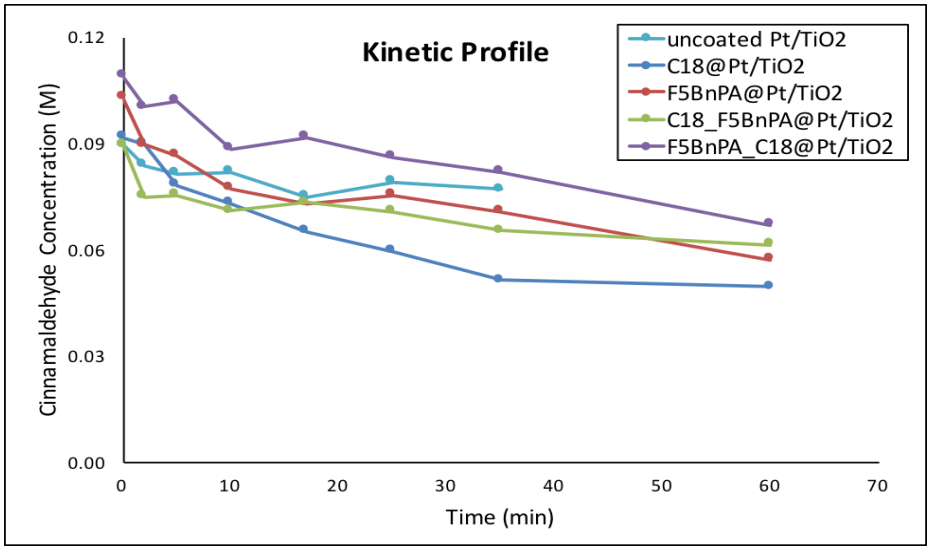

Figure 12: Reactant concentration over time.

When the rate was divided by the amount of catalyst present to calculate the overall turnover frequency and the turnover frequency for cinnamyl alcohol, the uncoated catalyst had significantly lower rates than the coated catalysts. For the titania support without modifiers, there was very low activity on

the surface to cinnamyl alcohol and all of the other products. Activity greatly increased when coatings were added to the surface.

The C18 increased the turnover frequency overall and for the cinnamyl alcohol production since the C18 helps to improve the amount of cinnamyl alcohol produced. The F5BnPA monolayer caused an increase in the overall turnover, but it had a lower increase for cinnamyl alcohol production. The phosphonate is not known to improve selectivity, so while it increased the activity, it was towards the other products in the reaction.

The largest increases in turnover frequency were from the dually coated catalysts. The phosphonate on the surface of each seemed to have a large impact on the activity. This activity increase was also large for the cinnamyl alcohol turnover since the C18 on the surface could block the terrace sites that more frequently produce hydrocinnamaldehyde.

The monolayers appeared to have a larger effect on the activity for the Pt/TiO_2 catalyst than the Pt/Al_2O_3. The alumina support was improved by the monolayers, but the increases in turnovers were larger on the titania surface, especially since the uncoated surface initially had a very low turnover frequency.

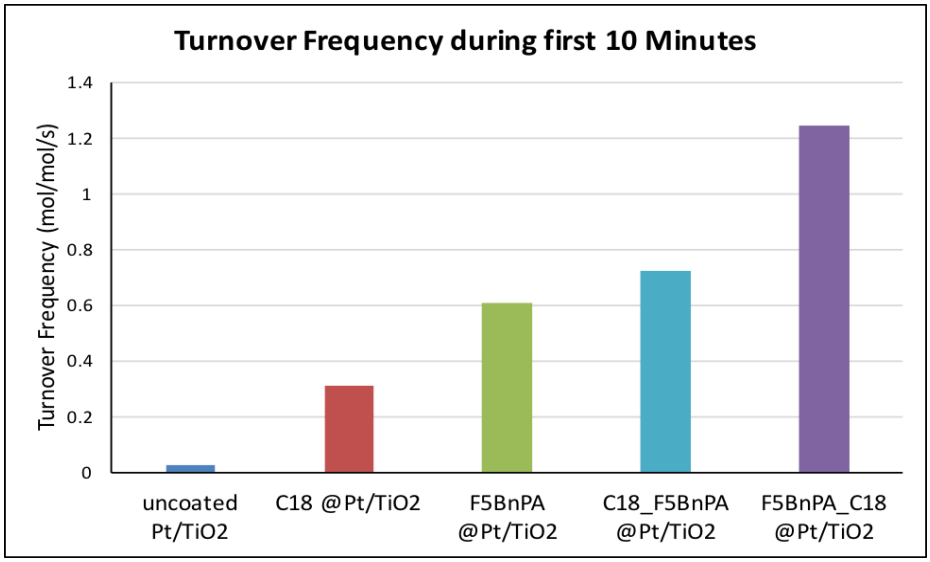

Figure 13: Overall turnover frequency on titania supported catalysts.

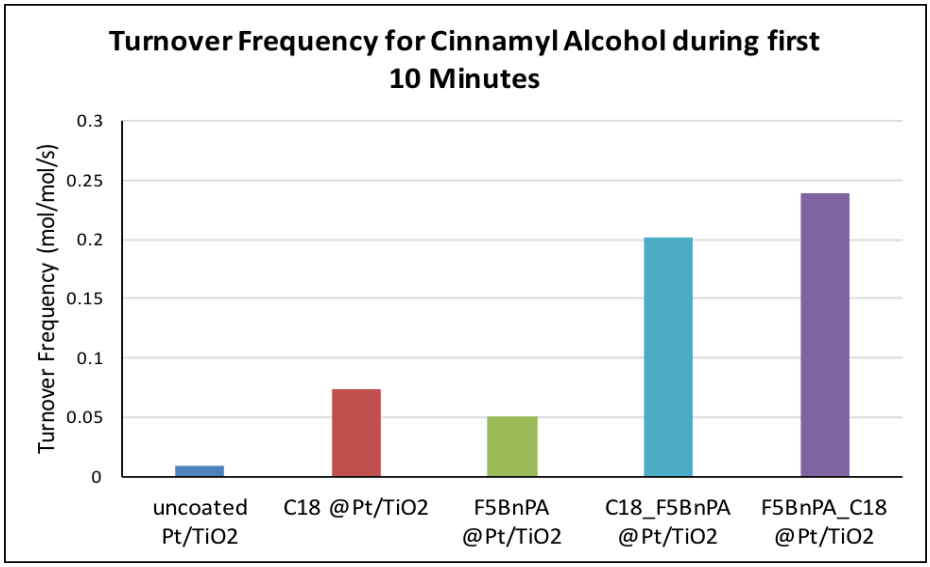

Figure 14: Turnover frequency for cinnamyl alcohol on titania supported catalyst.

Conclusions and Recommendations

Conclusions

Catalysts can be coated with both thiols and phosphonates from a sequential deposition of either order on Pd/Al_2O_3 and Pt/Al_2O_3. The order of deposition impacts both the selectivity and the activity of the reaction. The selectivity to cinnamyl alcohol was improved by C18, while lowered by F5BnPA. For the dually coated catalysts, the second coating added to the catalysts affected the selectivity more significantly. For the activity of the catalyst, the F5BnPA and the F5BnPA added after C18 had the highest reaction rates. When turnover frequency was calculated for cinnamyl alcohol specifically, the F5BnPA added after C18 had the highest rate; the C18 on the surface could open the desired active sites that would increase the selectivity to cinnamyl alcohol, while the F5BnPA increased the rate of this reaction.

Recommendations

Sequential depositions have been proven to be successful in depositing the thiol and phosphonate combination on Pd/Al_2O_3, Pt/Al_2O_3, Pd/TiO_2, Pt/TiO_2. To improve the versatility of this type of catalyst modification, other metals should be tested to see if the SAMs will both deposit onto the surface. Also, the metal oxide support could be changed to investigate its effect in combination with the SAMs.

Additionally, the thiol and phosphonates used in the combination could be changed to tune the catalyst more specifically for a certain reaction. For this study, the combination was used, since it was clear that both were attached to the surface. With other combinations, the structure of the tail could be used to further increase the selectivity by adding benzene rings in certain locations. Different

phosphonates could also be used that have a smaller tail so that there is less steric hindrance for the reaction, specifically at the edge sites on the interface.

Finally, reactions should all be done at higher pressure to increase the conversion within an hour, since the selectivity varies with conversion.

Chapter 3

Computational Single Atom Catalyst Study

Methods

Electronic Structure

Reaction energies and barriers for the hydrogenation of trans-2-butene and acetaldehyde were calculated with density functional theory using the Vienna Ab Initio Software Package (VASP) by Kresse and Hafner[18,19]. The reactions were carried out on a single atom catalyst (SAC) of Pt_1/TiO_2 anatase (101). The number of O on the surface were varied to model an adsorbed Pt^{4+}, Pt^{2+}, and Pt^0 (formal charge) species. The model had 5 layers of TiO_2 with the bottom 3 layers fixed during structural optimization and the remaining surface layers, Pt, and adsorbate positions optimized. The surface was modeled with a 2 by 4 surface cell, such that the unit cell had 40 TiO_2 units. All calculations used on the gamma point for kpoint sampling due to the large unit cell. All calculations were spin polarized. The calculations were considered optimized when the forces on all atoms were less than 0.05 eV/Å.

Catalyst Model

To model Pt^{4+} on the surface, PtO_2 was placed on the surface of the TiO_2 with the Pt atom centered over a subsurface Ti atom (Figure 15a/15b). The Pt bonded to the two oxygens placed on the surface along with one oxygen from the TiO_2 structure. The oxygen from the TiO_2 moved up from the structure to bind to the Pt, which remained centered over the subsurface Ti atom.

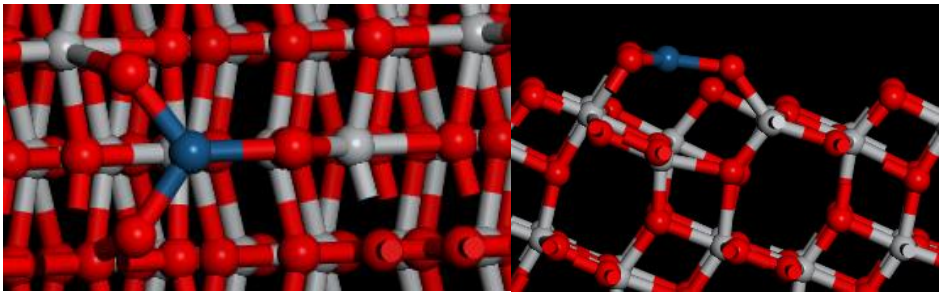

Figure 15a/15b: Top and side view of bare PtO2/TiO2 surface

One oxygen atom from the PtO_2 adsorbed structure was removed to model a formal Pt^{2+} species on the surface (Figure 16a/16b). In the optimized adsorbed PtO structure, the Pt atom was bound to both the oxygen added to the surface and an oxygen from the TiO_2. The Pt atom optimized to a position slightly offset from being directly above the Ti atom.

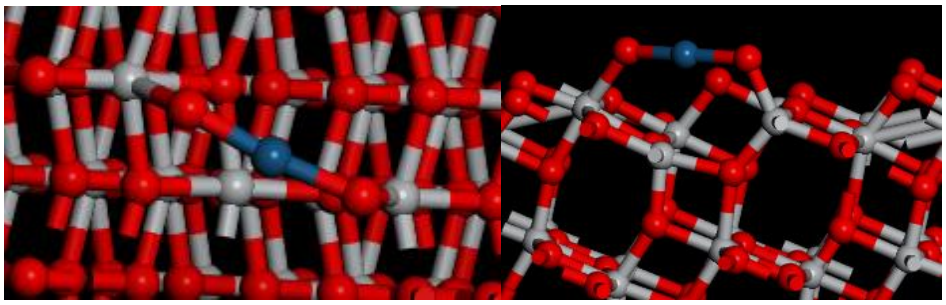

Figure 16a/16b: Top and side view of bare PtO/TiO2 surface

Another oxygen atom was removed from the adsorbed PtO species to model a formal Pt^0 adsorbed (Figure 17a/17b). The Pt atom remained bonded to one oxygen from the TiO_2, and the structure reorganized so that a a second oxygen from the surface that bridged the Pt atom and a surface Ti atom. The Pt atom moved closer to the TiO_2 surface in this model, with an indication that there is also a bonding interaction between the Pt atom and the Ti atom directly below.

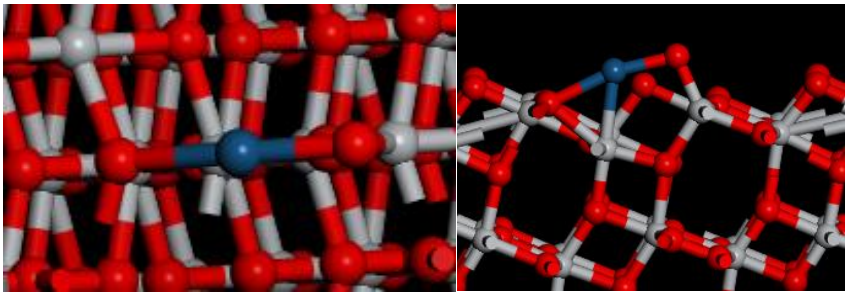

Figure 17a/17b: Top and side view of bare Pt/TiO2 surface

Hydrogenation Reaction Energy Calculations

The hydrogenation reaction was modeled by a sequence of elementary steps. First the initial reactant hydrocarbon adsorbed on the surface without the presence of the hydrogen, and the adsorption energy was calculated. A hydrogen atom is then adsorbed to the surface and the adsorption energy calculated relative to ½ of a H_2 molecule. The final state was then modeled by transferring the adsorbed H to the adsorbed reactor to form a hydrogenated intermediate adsorbed to the surface. The reaction energy is calculated by comparing the energy of the initial adsorbed reactant with hydrogen co-adsorbed to the final state. The bare Pt/TiO_2 surface and the adsorbed molecules (trans-2-butene and acetaldehyde) were optimized separately to obtain their individual energies. Relative energies were calculated between the different structures along the hydrogenation reaction pathway to determine the reaction energy of each step. To put all steps onto a reaction energy diagram, the relative energy of each state along the path was calculated by subtracting the energy of the bare surface and individual adsorbed molecules from the optimized reaction step structure.

Results and Discussion

Adsorption of Reactant Molecules

The first step modeled in the reaction mechanism was the adsorption of the reactant molecule to the surface. This step was completed for both trans-2-butene and acetaldehyde on the three oxidation states of TiO_2-adsorbed Pt (4+, 2+, 0). The step was modeled by calculating the lowest energy structure of the molecule adsorbed to the surface and comparing it to the energy of the bare surface and separate reactant to determine the adsorption energy.

For trans-2-butene, the strongest adsorption occurred on Pt^0 and the weakest on Pt^{2+}. The trans-2-butene was favorably adsorbed (adsorption energy was negative) to the Pt atom on all three surfaces (Figure 18a/18b). Structurally, the two double-bonded carbons (C_2 and C_3) both bonded to the Pt atom, adsorbing through a pi-bond interaction with the Pt atom. The C=C substituents remained approximately planar in all adsorbed structures, suggesting the carbons remained sp^2 hybridized. The position of the Pt atom moved in all three structures from sitting over a Ti atom to moving over an oxygen atom where a Pt-O bond was present. With butene adsorbed, the Pt^{4+} and the Pt^{2+} both remain bound to the superstoichiometric oxygen atoms.

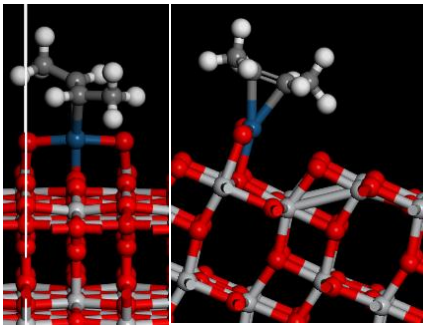

Figure 18a/a8b: Trans-2-butene adsorbed on PtO_2/TiO_2

In the model of acetaldehyde adsorption, the most stable adsorption was again to the Pt^0, and again the least favorable adsorption was to the Pt^{2+}. On the three surfaces, the adsorption occurred through the C=O pi-bond and the Pt atom, and the C atom remained sp^2 hybridized. The placement of the

Pt atom also shifted to be above an oxygen atom from the TiO_2. The Pt was bonded to the oxygen below, along with the superstoichiometric oxygen present in the Pt^{2+} and the Pt^{4+} models (Figure 19a/19b). The adsorption of the molecule was favorable on all 3 surfaces.

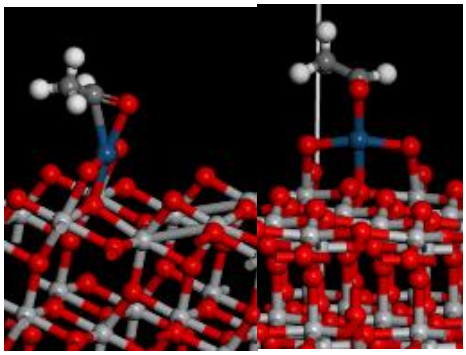

Figure 19a/19b: Adsorbed acetaldehyde on PtO_2/TiO_2

Both model reactants adsorbed favorably on all three catalysts, showing that this step of the reaction mechanism is favorable (Figure 20/21). The favorable adsorption ensures that the desired reactant will interact with the catalyst, and Pt, PtO, and PtO_2 structures all expose a Pt coordination site capable of binding to alkenes or carbonyl groups with adsorption energies ranging from ~-0.5 to -2 eV. Comparatively between the two molecules, trans-2-butene adsorbed stronger to all the surfaces. This could indicate that a reactant, such as cinnemaldehyde, that has both C=C and C=O bonds would preferentially bind through the C=C function.

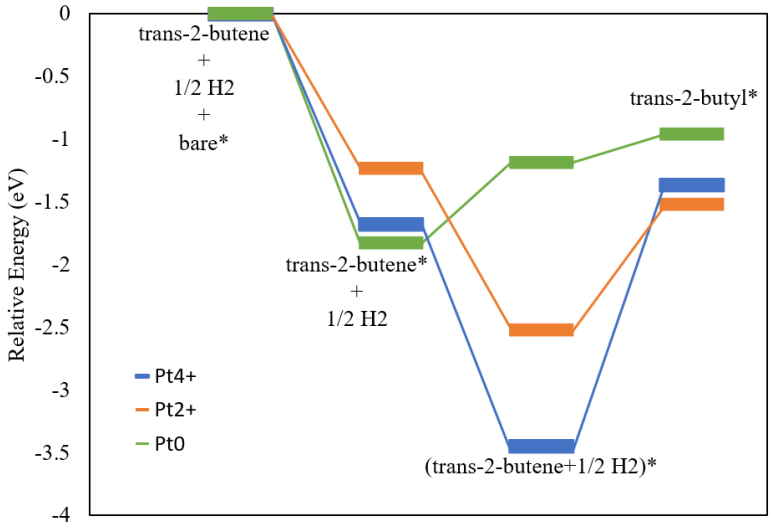

Figure 20: Relative energy comparison of reaction pathway for trans-2-butene hydrogenation

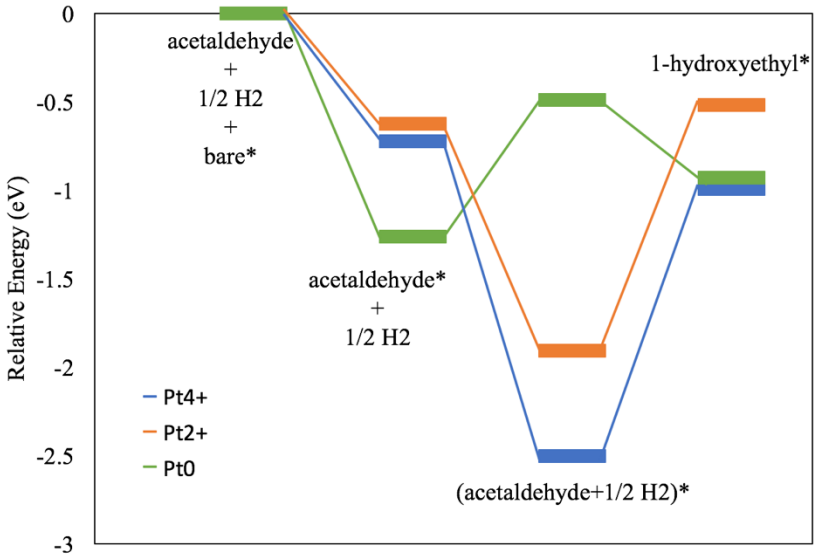

Figure 21: Relative energy comparison of reaction pathway for acetaldehyde hydrogenation

Adsorption of Hydrogen

The next step within the hydrogenation mechanism is the adsorption of a hydrogen atom on the surface. Hydrogen was adsorbed in multiple locations, including on the Pt atom and to non-symmetry equivalent surrounding oxygens, to find the lowest energy structure when co-adsorbed with the reactant

molecule (Figure 22a, 22b, 22c). The lowest energy structure is reported, and is used in reaction energy calculations as it is the most probable position of a hydrogen atom on the surface. Very similar trends were observed for both the trans-2-butyl and acetaldehyde. The lowest energy co-adsorbed structure for the Pt^{2+} and Pt^{4+} models had the hydrogen bonded to one of the superstoichiometric oxygen atoms for both the acetaldehyde and trans-2-butyl. For the trans-2-butyl system, hydrogen on this oxygen, which is also interacting with Pt, is more favorable by 0.39 eV compared to a H-adsorption to an oxygen in the TiO_2. When the hydrogen was initially placed on the Pt atom, it would move to the nearby oxygen to reach a lower energy structure. H* adsorption on the PtO and PtO_2 models was favorable with respect to gas phase H_2, with adsorption stronger the more oxidized the Pt atom was. Adsorption to the PtO_2 structure was extremely favorable (order -2 eV relative to ½ H_2), suggesting an even greater coverage of H* might be established on this surface. Consideration of higher H* coverages is left for future work.

On the Pt^0 surface, the hydrogen bonded to an oxygen in the TiO_2 since there were no added surface oxygen in that system.

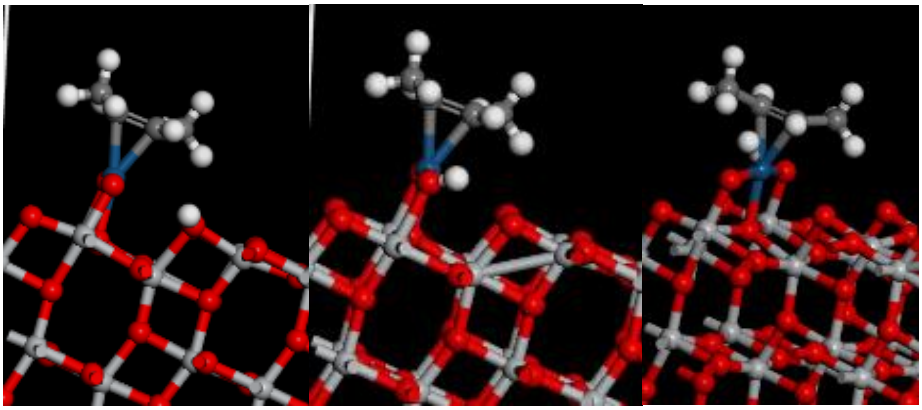

Figure 22a/22b/22c: Hydrogen adsorbed on surface oxygen, added oxygen, and Pt atom

Pt^0 does not have any additional oxygen on the surface, making H* bond to a less favorable oxygen within the TiO_2 structure. The addition of the hydrogen in the Pt^0 is unfavorable to the extent that the new structure is at a higher energy than when just the trans-2-butene or acetaldehyde is adsorbed. The adsorption energy was 0.64 eV for the trans-2-butene and 0.77 eV for the acetaldehyde, suggesting the full-reduced Pt atom cannot be further reduced by H adsorption. The positive adsorption energy makes it

unlikely that hydrogen would bond to the surface to be able to complete the hydrogenation reaction on the Pt^0 catalyst for either of the molecules.

H and the C=C or C=O containing species will not co-adsorb directly on the Pt atom, regardless of Pt oxidation state. Therefore, hydrogenation will require transferring a H* adsorbed to an O atom of the PtO or PtO_2 species to a C atom interacting with Pt.

Hydrogenation

To model the final step for the reaction, where the hydrogenation (C-H bond formation) takes place, the product molecule was adsorbed on the Pt/TiO_2 surfaces. When hydrogenating trans-2-butene, the lowest energy product structure was formed on the Pt^{2+}, followed by Pt^{4+} (Figure 23a/23b). However, there was a positive reaction energy for the hydrogenation step for both the Pt^{4+} and Pt^{2+} catalysts. The positive reaction energies of 2.08 eV for the Pt^{4+} and 1.00 eV for the Pt^{2+} mean that the elementary hydrogenation reaction is unfavorable on the catalyst, and suggest that further consideration of higher H* coverages is warranted. Specifically, in both cases the hydrogen on the surface was adsorbed very strongly to the surface, which would make it difficult for the hydrogen to leave the surface. On all surfaces, the formation of adsorbed butyl is favorable relative to the isolated trans-2-butene molecule and ½ H_2. On Pt^{2+}, product formation is also favorable relative to adsorbed trans-2-butene and ½ H_2. These results suggest that hydrogenation could be a favorable surface process, though we have not arrived at an elementary model of H adsorption and the hydrogenation step that would show feasible energetics of all elementary steps.

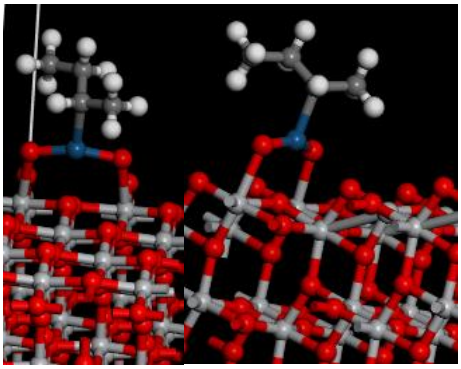

Figure 23a/23b: Hydrogenated trans-2-butene (trans-2-butyl) adsorbed on PtO2/TiO2

The hydrogenation of acetaldehyde also produced similar results (Figure 24a/24b). The most stable final state was the Pt^{4+}, but the reaction energy for that model was 1.51 eV, making the reaction unfavorable. The Pt^{2+} had the highest energy final state along with a reaction energy of 1.39 eV so it would be unlikely for this model to hydrogenate acetaldehyde. The overall reaction energy for this first hydrogenation step is favorable relative to gas phase acetaldehyde and gas phase ½ H_2 on all models, and is favorable relative to the adsorbed acetaldehyde state (and gas phase ½ H_2) on the Pt^{4+} model.

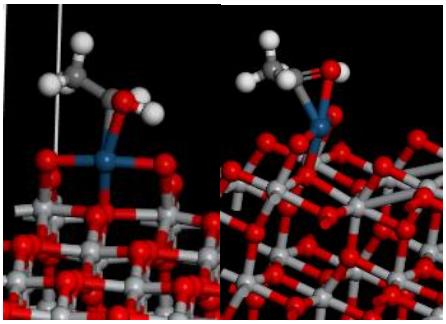

Figure 24a/24b: Hydrogenated acetaldehyde on PtO_2/TiO_2

Finally, the Pt^0 had the smallest barrier of 0.23 eV for trans-2-butene hydrogenation and had a favorable reaction energy of -0.43 eV for acetaldehyde hydrogenation. However, this catalyst had the most unstable structure for the adsorption of hydrogen. Since it is unlikely that

hydrogen would adsorb to the Pt^0 surface, the hydrogenation reaction would not occur on this catalyst.

Comparing the hydrogenation of the two molecules, acetaldehyde reacts more favorably on the Pt^{4+} catalyst than trans-2-butene, since the reaction energy is lower. Conversely, the hydrogenation of trans-2-butene is more favorable on the Pt^{2+} catalyst than the hydrogenation of acetaldehyde.

Experimentally, Pt/TiO_2 catalysts can hydrogenate both carbon-carbon double bonds and carbon-oxygen double bonds using the nanoparticle catalysts presented earlier. The Medlin and Christopher (UCSB) groups have also observed that single atom Pt on TiO_2 can hydrogenate both of these bond types. The computational results indicate specific reaction steps are unfavorable in the mechanism considered, so there is most likely something missing from the computational model to better show what occurs experimentally. The SAC computational model is different than a Pt nanoparticle catalyst, and should not be expected to exactly capture energetics on such catalysts. These results, however, show that there are more modeling factors that must be considered for hydrogenation of these molecules for single atom Pt on TiO_2.

Conclusions and Recommendations

Conclusions

The adsorption of the reactant molecules, trans-2-butene and acetaldehyde, was favorable on the three oxidation states of Pt modeled. The hydrogen adsorbs favorably to the added oxygen on the surface of Pt^{4+} and Pt^{2+} for both molecules. However, the adsorption of hydrogen is unfavorable on Pt^{0}, preventing the Pt^{0} catalyst from having the hydrogen present to hydrogenate trans-2-butene and acetaldehyde. Hydrogenation of trans-2-butene and acetaldehyde is unfavorable on both the Pt^{2+} and Pt^{4+}, as H* adsorption appears to be too favorable on these models. This result motivates consideration of greater adsorbed H* coverages on the oxidized Pt models. Pt^{4+} favors the hydrogenation of acetaldehyde and Pt^{2+} favors the hydrogenation of trans-2-butene.

Recommendations

More work should be done on the computational model of the Pt/TiO_2 SAC to align results more similarly to the experimental results. Higher hydrogen coverage on the different catalysts should be modeled to add hydrogen to the surface that is less strongly bonded, so that the final hydrogenated state is more favorable comparatively. Self-Assembled Monolayers could be investigated, like those used experimentally. These could have the potential to block hydrogen from bonding to the extremely low energy sites that make the hydrogenation unfavorable. Additionally, other model molecules with carbon-carbon and carbon-oxygen double bonds could be tested to see if there is a better way to model the hydrogenation of cinnamaldehyde computationally. Finally, when a better model is produced, the 2nd hydrogenation of the reactant molecules should be modeled to show the full hydrogenation of the double bonds.

BIBLIOGRAPHY

1. Arai, M.; Obata, A.; Usui, K.; Shirai, M.; Nishiyama, Y. Activity for liquid-phase hydrogenation of α,β-unsaturated aldehydes of supported platinum catalysts prepared through low-temperature reduction. *Appl. Catal. A Gen*. **1996**, *146(2)*, 381-389.
2. Schoenbaum, C. A.; Schwartz, D. K.; Medlin, J. W. Controlling surface crowding on a Pd catalyst with thiolate self-assembled monolayers. *Journal of Catalysis*. **2013**, *303*, 92–99.
3. Wang, A.; Li, J.; Zhang, T. Heterogeneous single-atom catalysis. *Nature Reviews Chemistry*. **2018**, *2*, 65-81.
4. Schoenbaum, C. A.; Schwartz, D. K.; Medlin, J. W. Controlling the Surface Environment of Heterogeneous Catalysts Using Self-Assembled Monolayers. *Acc. Chem. Res.* **2014**, *47*, 1438−1445.
5. Kahsar, K. R.; Schwartz, D. K.; Medlin, J. W. Control of Metal Catalyst Selectivity through Specific Noncovalent Molecular Interactions. *J. Am. Chem. Soc*. **2014**, *136*, 520−526.
6. Hotchkiss, P. J.; Malicki, M.; Giordano, A. J.; Armstrong, N. R.; Marder, S. R. Characterization of phosphonic acid binding to zinc oxide. *J. Mater. Chem*. **2011**, *21*, 3107–3112.
7. Sang, L.; Mudalige, A.; Sigdel, A. K.; Giordano, A. J.; Marder, S. R.; Berry, J. J.; Pemberton, J. E. PM-IRRAS Determination of Molecular Orientation of Phosphonic

Acid Self-Assembled Monolayers on Indium Zinc Oxide. *Langmuir.* **2015**, *31*, 5603−5613.

8. Ellis, L. D.; Pylypenko, S.; Ayotte, S. R.; Schwartz, D. K.; Medlin, J. W. Trimethylsilyl functionalization of alumina (γ-Al2O3) increases activity for 1,2-propanediol dehydration. *Catal.Sci.Technol*. **2016**, *6*, 5721-5728.
9. Pujari, S. P.; Scheres, L.; Marcelis, T. M.; Zuilhof, H. Covalent Surface Modification of Oxide Surfaces. *Angew. Chem. Int. Ed*. **2014**, *53*, 6322 – 6356.
10. Gallezot, P.; Richard, D. Selective Hydrogenation of α,β-Unsaturated Aldehydes. *Catalysis Reviews*. **1998**, *40:1-2*, 81-126.
11. Weissermel, K.; Arpe, H. *J. Industrial Organic Chemistry*, Verlag Chemie, Weinheim, **1978**.
12. Bauer, K.; Garbe, D. Common Fragrance and Flavor Materials, VCH, Weinheim, 1985 Wagner, M.; Kohler, K.; Djakovitch, L.; Weinkauf, S.; Hagen, V.; Muhler, M. Heck reactions catalyzed by oxide-supported palladium – structure–activity relationships. *Topics in Catalysis*, **2000**, *13*, 319–326.
13. DeRita, L.; Dai, S.; Lopez-Zepeda, K.; Pham, N.; Graham, G. W.; Pan, X.; Christopher, P. Catalyst Architecture for Stable Single Atom Dispersion Enables Site Specific Spectroscopic and Reactivity Measurements of CO Adsorbed to Pt Atoms, Oxidized Pt Clusters, and Metallic Pt Clusters on TiO2. *J. Am. Chem. Soc*, **2017**, 139, 14150-14165.
14. Matsubu, J. C,; Yang, V. N.; Christopher, P. Isolated Metal Active Site Concentration and Stability Control Catalytic CO_2 Reduction Selectivity. *J. Am. Chem. Soc.*, **2015**, *137* (8), 3076–3084.

15. Zhang, X.; Shi, H.; Xu, B. Catalysis by Gold: Isolated Surface Au^{3+} Ions are Active Sites for Selective Hydrogenation of 1,3-Butadiene over Au/ZrO_2 Catalysts. *Angewandte Chemie*, **2005**, *114* (43), 7294-7297.

16. Kyriakou, G.; Boucher, M. B.; Jewell, A. D.; Lewis, E. A.; Lawton, T. J.; Baber, A. E.; Tierney, H. L.; Flytzani-Stephanopoulos, M.; Sykes E. Isolated Metal Atom Geometries as a Strategy for Selective Heterogeneous Hydrogenations. *Science*, **2012**, *335*, 1209-1212.

17. Vilé, G.; Albani, D.; Nachtegaal, M.; Chen, Z.; Dontsova, D.; Antonietti, M.; López , N.; Pérez-Ramírez, J. A Stable Single-Site Palladium Catalyst for Hydrogenations. *Angew. Chem. Int. Ed.*, **2015,** *54*, 11265-11269.

18. Kresse, G.; Furthmuller, J., Efficiency of Ab-Initio Total Energy Calculations for Metals and Semiconductors Using a Plane-Wave Basis Set. *Comp. Mater. Sci.* **1996**, *6*, 15-50.

19. Kresse, G.; Joubert, D., From Ultrasoft Pseudopotentials to the Projector Augmented-Wave Method. *Phys. Rev. B* **1999**, *59*, 1758-1775.

ACADEMIC VITA

MEGAN INGALLS

EDUCATION

Bachelor of Science in Chemical Engineering **Graduation: May 2019**
Schreyer Honors College
The Pennsylvania State University, University Park, PA

Mechanical Engineering Product Design Program **May 2016**
National University of Singapore, Singapore

EMPLOYMENT

Phillips 66- Process Control Intern **May 2018-August 2018**

- Assisted in DCS system upgrade
- Transferred PLC logic to DCS
- Converted and implemented new PI graphics to match DCS system

Phillips 66- Process Engineering Intern **May 2017-August 2017**

- Monitored Process Units Daily to ensure proper performance
- Proved a cost savings measure feasible and created project proposal for a savings of $200k per year
- Evaluated refinery air system and provided recommendations for reliability

Kimberly Clark- Process Engineering Co-op **Jan 2017-May 2017**

- Lead a manufacturing trial to test and optimize a new process to reduce cost
- Evaluated the reliability of a new process to save capital for a project
- Participated on multidisciplinary capital project team by completing various design and engineering tasks

RESEARCH

Undergraduate Research Assistant **Jan 2016- Present**
Michael Janik Research Group

- Use computational tools to build self-assembled monolayer coated surfaces
- Investigate the tail interactions between different self-assembled monolayers

Colorado Center for Biorefining and Bioproducts REU **Summer 2016**

- Prepared a dually coated heterogeneous catalyst
- Tested the effects of both phosphonates and thiols on a catalytic surface
- Awarded 2nd place in Catalysis & Reaction Engineering III at AIChE Annual Student Conference

ACTIVITIES

Engineering Undergraduate Council, Outreach Chair **Aug 2016-May 2017**